Structural analysis of the stalk subunit Vma5p of the yeast V-ATPase in solution

Andrea Armbrüster[a], Dmitri I. Svergun[b], Ünal Coskun[a], Sandra Juliano[a], Susanne M. Bailer[c], Gerhard Grüber[a,*]

[a] *Universität des Saarlandes, Fachrichtung 2.5 – Biophysik, Universitätsbau 76, D-66421 Homburg, Germany*
[b] *European Molecular Biology Laboratory, Hamburg Outstation, EMBL c/o DESY, D-22603 Hamburg, Germany*
[c] *Universität des Saarlandes, Fachrichtung 2.3 – Medizinische Biochemie und Molekularbiologie, D-66421 Homburg, Germany*

Received 26 May 2004; revised 9 June 2004; accepted 10 June 2004

Available online 21 June 2004

Edited by Stuart Ferguson

Abstract Vma5p (subunit C) of the yeast V-ATPase was produced in *Escherichia coli* and purified to homogeneity. Analysis of secondary structure by circular dichroism spectroscopy showed that Vma5p comprises 64% α-helix and 17% β-sheet content. The molecular mass of this subunit, determined by gel filtration analysis and small angle X-ray scattering (SAXS), was approximately 51 ± 4 kDa, indicating a high hydration level of the protein in solution. The radius of gyration and the maximum size of Vma5p were determined to be 3.74 ± 0.03 and 12.5 ± 0.1 nm, respectively. Using two independent ab initio approaches, the first low-resolution shape of the protein was determined. Vma5p is an elongated boot-shaped particle consisting of two distinct domains. Co-reconstitution of Vma5p to V_1 without C from *Manduca sexta* resulted in a V_1–Vma5p hybrid complex and a 20% increase in ATPase hydrolysis activity.

Keywords: Vacuolar-type ATPase; V_1V_O ATPase; V_1 ATPase; Vma5p; F-ATPase; Circular dichroism spectroscopy; Small angle X-ray scattering

1. Introduction

The Vacuolar ATPase (V_1V_O ATPase) is an electrogenic ion pump found throughout every eukaryotic cell. This enzyme harnesses the energy derived from ATP hydrolysis to pump ions across membranes, creating an electrochemical gradient. As suggested by its bipartite name, the V_1V_O ATPase is composed of a water-soluble V_1 ATPase and an integral membrane subcomplex, V_O. ATP is hydrolyzed on the V_1 headpiece consisting of an A_3:B_3 hexamer, and the energy released during that process is transmitted to the membrane-bound V_O domain, to drive the ion translocation. This energy coupling occurs via the so-called ''stalk'' structure, an assembly of the V_1 subunits C–H, respectively, that forms the functional and structural interface [1–3]. The proposed subunit stoichiometry of V_1 is A_3:B_3:C_1:D_1:E_1:F_1:G_2:H_x [4]. The integral V_O domain contains five different subunits in a stoichiometry of a_1:d_1:c_{4-5}:c'_1:c''_1 [5].

Low-resolution structural studies of the V_1 ATPase from *Manduca sexta* using small angle scattering have shown that the hydrated V_1 is rather elongated, with a headpiece of 14.5 nm in diameter and a stalk of approximately 11 nm in length [6]. Previously, we have obtained a three-dimensional structure of this V_1 ATPase without subunit C at 1.8 nm resolution [7]. This showed that the A_3 and B_3 subunits alternate in a hexagonal arrangement and that the stalk region protrudes by approximately 6 nm from the surface of the A_3B_3 headpiece. Understanding the structural and functional roles of the V-ATPase stalk and its subunits is essential, because they may impart to V-ATPases the characteristics that distinguish them from the F-ATPases. These include their activity as dedicated ion pumps rather than ion-driven ATP synthases, and their susceptibility to multiple forms of regulation in vivo like the reversible reassembly of the V_1 and V_O domains, which results in silencing of both parts [8–10]. The stalk subunits C and H have been proposed to be involved in silencing of Mg-activated ATP hydrolysis [11]. Subunit H (Vma13p) from yeast has recently become the first eukaryotic V-ATPase subunit to have a crystal structure solved [12]. This subunit is characterized by the large primarily α helical N-terminal domain, forming a shallow groove, and the C-terminal domain, both connected by a four-residue loop. The elongated shape of subunit H enables this subunit to contact both the catalytic A subunit and subunit a, thereby bridging the V_1 headpiece with the membrane bound V_O portion [13]. We have turned our attention to the examination of subunit C (Vma5p) from yeast and describe here the production of subunit C (Vma5p) and the analysis of its secondary and quaternary structure in solution using circular dichroism spectroscopy (CD) and small angle X-ray scattering (SAXS), respectively. (Note, the crystal structure of subunit C of the bacterial A_1A_O ATPase from *Thermus thermophilus* has recently been determined [14]. This subunit is homologous to subunit d (Vma6p) of the yeast V-ATPase [15]).

2. Materials and methods

2.1. Biochemicals

ProofStart™ DNA Polymerase and Ni^{2+}–nitrilotriacetic acid (NTA) chromatography resin were received from Qiagen (Hilden, Germany); restriction enzymes were purchased from MBI Fermentas

* Corresponding author. Fax: +49-6841-1626086.
E-mail address: ggrueber@med-rz.uni-saarland.de (G. Grüber).

Abbreviations: BSA, bovine serum albumin; IPTG, isopropyl-β-D-thiogalactoside; NTA, nitrilotriacetic acid; PAGE, polyacrylamide gel electrophoresis; PCR, polymerase chain reaction; SDS, sodium dodecyl sulfate; Tris, Tris-(hydroxymethyl)aminomethane

0014-5793/$22.00 © 2004 Federation of European Biochemical Societies. Published by Elsevier B.V. All rights reserved.
doi:10.1016/j.febslet.2004.06.029

(St. Leon-Rot, Germany). The expression vector pET9d-His_6 was provided by G. Stier, EMBL (Heidelberg, Germany). Chemicals for gel electrophoresis were received from Serva (Heidelberg, Germany). Bovine serum albumin (BSA) was purchased from GERBU Biochemicals (Heidelberg, Germany). All other chemicals were at least of analytical grade and received from BIOMOL (Hamburg, Germany), Merck (Darmstadt, Germany), Roth (Karlsruhe, Germany), Sigma (Deisenhofen, Germany), or Serva (Heidelberg, Germany).

2.2. Production and purification of Vma5p (subunit C)

To amplify the *VMA5* coding region, oligonucleotide primers 5′-CATGCCATGGCTACTGCGTTATATA-3′ (forward primer) and 5′-CGGGATCCTTATAAATTGATTATATACAT-3′ (reverse primer), incorporating *Nco*I and *Bam*HI restriction sites, respectively (underlined), were designed. *Saccharomyces cerevisiae* genomic DNA was used as template for the polymerase chain reaction (PCR). Following digestion with *Nco*I and *Bam*HI, the PCR product was ligated into the pET9d-His_6 vector. The pET9d-His_6 vector containing the *VMA5* insert was then transformed into *E. coli* cells (strain BL21) and grown on 30 μg/ml kanamycin-containing Luria–Bertoni (LB) agar plates. To express His_6-Vma5p, liquid cultures were shaken in LB medium containing kanamycin (30 μg/ml) for about 20 h at 30 °C until an optical density OD_{600} of 0.6–0.7 was reached. To induce production of His_6-Vma5p, the cultures were supplemented with isopropyl-β-D-thiogalactoside (IPTG) to a final concentration of 1 mM. Following incubation for another 4 h at 30 °C, the cells were harvested at $10\,000 \times g$ for 20 min, 4 °C. Subsequently, they were lysed on ice by sonication for 3×1 min in buffer A (50 mM Tris-(hydroxymethyl)aminomethane (Tris)/HCl, pH 8.5, 100 mM NaCl, and 8 mM Pefabloc SC (BIOMOL)). The lysate was cleared by centrifugation at $10\,000 \times g$ for 30 min at 4 °C, the supernatant was passed through a filter (0.45 μm pore-size) and supplemented with Ni^{2+}–NTA resin. The His-tagged protein was allowed to bind to the matrix for 90 min at 4 °C and eluted with an imidazole gradient (25–200 μM) in buffer A by mixing on a sample rotator (Neolab). Fractions containing His_6-Vma5p/subunit C were identified by sodium dodecyl sulfate–polyacrylamide gel electrophoresis (SDS–PAGE)[1] [16], pooled and concentrated using Centriprep YM-10 (10 kDa molecular mass (MM) cut off) spin concentrators (Millipore) and subsequently applied on an ion-exchange column (Resource Q (6 ml), Amersham Biosciences), equilibrated in a buffer of 50 mM Tris/HCl (pH 8.5), 100 mM NaCl and 1 mM DTT[1]. The purity of the protein sample was analyzed by SDS–PAGE. The SDS-gels were stained with Coomassie Brilliant Blue G250. Protein concentrations were determined by the bicinchonic acid assay (BCA; Pierce, Rockford, IL. USA). For the N-terminal sequencing, subunit C (Vma5p) was blotted on a polyvinylidene difluoride membrane (pore size 0.45 μm) according to [17]. The protein bands were excised from the membrane and sequenced with a model 473A sequencer from Applied Biosystems.

2.3. Determination of native molecular mass

Gel filtration chromatography was performed using a Superdex 75 HR 10/30 column (Amersham Biotech) using a buffer of 50 mM Tris/HCl (pH 8.5), 100 mM NaCl and 1 mM DTT. To construct a calibration curve, a set of standard proteins (Amersham Biotech and Sigma) was analyzed. The K_{av} parameter was determined ($K_{av} = (V_e - V_0)/(V_t - V_0)$, where V_e represents the elution volume, V_0 the void volume, and V_t the total bed volume). The K_{av} values for standard proteins were plotted as a function of the logarithm of molecular mass (MM) and the resulting calibration curve was used to derive the MM of Vma5p (subunit C).

2.4. CD spectroscopy

A Jasco-715 spectropolarimeter fitted with a Jasco-PTC348 temperature controller was used for CD experiments. Spectra were collected in 0.1 mm quartz cells (Hellma) at 10 °C between 190 and 250 nm at a step resolution of 0.2 nm. CD spectroscopy of subunit C (1.0 mg/ml) was performed in 50 mM Tris/HCl, pH 8.5, 100 mM NaCl and 1 mM DTT using 0.5 nm path length. Ten scans were averaged to obtain a final spectrum. The spectrum for the buffer was subtracted from the spectrum of subunit C. This baseline corrected spectrum was used as input for computer methods to obtain predictions of secondary structure. In order to analyze the CD spectrum, the analysis programs Contin [18] and K2D [19] were used.

2.5. X-ray scattering experiments and data analysis of Vma5p (subunit C)

The synchrotron radiation X-ray scattering data were collected following standard procedures on the X33 camera [20,21] of the EMBL on the storage ring DORIS III of the Deutsches Elektronen Synchrotron (DESY) using multiwire proportional chambers with delay line readout [22]. The scattering patterns from subunit C at protein concentrations of 2.9, 5.9, 11.8 and 27.9 mg/ml were measured using a two-detector setup with the sample–detector distances of 2.2 and 1.2 m, covering a range of momentum transfer $0.15 < s < 9.8$ nm^{-1} ($s = 4\pi\sin(\theta)/\lambda$, where θ is the scattering angle and $\lambda = 0.15$ nm is the X-ray wavelength). The data were normalized to the intensity of the incident beam and corrected for the detector response; the scattering of the buffer was subtracted and the difference curves were scaled for concentration. The low angle data measured at lower protein concentrations were extrapolated to infinite dilution and merged with the higher angle data to yield the final composite scattering curves. All the data processing steps were performed using the program package PRIMUS [23]. The maximum dimension of the subunit C, D_{max}, was estimated using the orthogonal expansion program ORTOGNOM [24]. The forward scattering $I(0)$ and the radius of gyration R_g were evaluated using the Guinier approximation [25] assuming that at very small angles ($s < 1.3/R_g$) the intensity is represented by $I(s) = I(0)\exp(-(sR_g)^2/3)$. These parameters were also computed from the entire scattering patterns using the indirect transform package GNOM [26], which also provides the distance distribution function $p(r)$ of the particle. The MM of subunit C was calculated by comparison with the forward scattering from the reference solution of BSA[1].

Low resolution models of the C subunit were built using two ab initio methods. The program DAMMIN [27] represents the protein shape as an ensemble of $M \gg 1$ densely packed beads inside a search volume (a sphere of diameter D_{max}). Each bead belongs either to the protein (index = 1) or to the solvent (index = 0), and the shape is thus described by a binary string of length M. Starting from a random string, simulated annealing [28] is employed to find a compact configuration of beads minimizing the discrepancy between the experimental $I_{exp}(s)$ and the calculated $I_{calc}(s)$ curves:

$$\chi^2 = \frac{1}{N-1}\sum_j \left[\frac{I_{exp}(s_j) - cI_{calc}(s_j)}{\sigma(s_j)}\right]^2, \quad (1)$$

where N is the number of experimental points, c is a scaling factor and $\sigma(s_j)$ is the experimental error at the momentum transfer s_j. The X-ray scattering curves at higher angles (starting approximately from $s = 2.5$ nm^{-1}) contain significant contribution from the internal particle structure which must be removed prior to the shape analysis. For this, a constant given by the slope of an $s^4I(s)$ versus s^4 plot is subtracted from the experimental data to ensure that the intensity would decay as s^{-4} following Porod's law [29] for homogeneous particles. The resulting "shape scattering" curve (i.e., scattering due to the excluded volume of the particle with unit density) in the range up to $s = 3.2$ nm^{-1} was used for ab initio shape restoration. The excluded volume of the hydrated particle (Porod volume) was computed from the shape scattering curve using the equation [29]

$$V = 2\pi^2 I(0)/\int_0^\infty s^2 I(s)\mathrm{d}s. \quad (2)$$

In a more versatile ab initio approach implemented in the program GASBOR [30], the protein is represented as a collection of dummy residues (DRs). Starting from randomly positioned residues, a chain-compatible spatial distribution of DRs inside the search volume is found by simulated annealing. The DR method permits to fit data up to 0.5 nm resolution but the number of residues must be known a priori. About a dozen DAMMIN and GASBOR reconstructions were performed and the independent models were analyzed using the package DAMAVER [31]. This package aligns all possible pairs of models using the program SUBCOMB [32] and identifies the most probable model giving the smallest average discrepancy with the rest. Moreover, the averaged model is computed by aligning all other models with the most probable one, computing the density map of beads and drawing the threshold corresponding to the excluded particle volume.

The scattering from the high resolution model of the regulatory subunit H of the V-ATPase of *S. cerevisiae* [12] was calculated from its structure deposited in the Brookhaven Protein Data Bank [33] (entry

1HO8) using the program CRYSOL [34]. Given the atomic co-ordinates, the program fits the experimental scattering curve by adjusting the excluded volume of the particle and the contrast of the hydration layer surrounding the particle in solution to minimize discrepancy [1] between the calculated and the experimental intensities.

2.6. Purification of the V_1(-C) ATPase from M. sexta and assembly with subunit C (Vma5p)

Tobacco hornworms were reared as described in [35]. The Manduca eggs were a generous gift of Dr. J. Schachtner, Philipps University in Marburg and Prof. Trenczek, University of Giessen, Germany. The V_1(-C) ATPase from *M. sexta* was isolated according to Rizzo et al. [35]. To remove 2-mercaptoethanol, the protein was dialyzed in a QuixSep™ Micro Dialyzer (Roth, Germany) for 6 h against a degassed buffer containing 20 mM Tris/HCl, pH 8.1, and 150 mM NaCl using a 10 kDa Spectra/Por dialysis membrane (*Spectrum Laboratories, Canada*). The protein was mixed with subunit C (Vma5p) overnight on a sample rotator at 4 °C. The incubated mixture was applied on a Sephacryl S-300 HR column with 20 mM Tris/HCl (pH 8.1), 150 mM NaCl. The peak fractions were collected and analyzed by SDS–PAGE. ATPase activity was measured as described previously [36].

3. Results

3.1. Purification of subunit C (Vma5p)

Induction of His-tagged protein production under the conditions specified in Section 2 resulted in an approximately 45 kDa protein which was found entirely within the soluble fraction. A Ni^{2+}–NTA resin column and an imidazole gradient (25–200 μM) in buffer consisting of 50 mM Tris/HCl, pH 8.5, and 100 mM NaCl was used to separate His_6-Vma5p/subunit C from the main contaminating proteins. Subunit C eluted at 100 mM imidazol was collected and subsequently applied to a RESOURCE™ Q column (Fig. 1). Analysis of the isolated protein by SDS–PAGE revealed the high purity of the protein. N-terminal sequence analysis was used to identify the protein as subunit C and its N-terminal His-tag (H H H H H H M A T A L Y T A N D F I L I S L P Q N A).

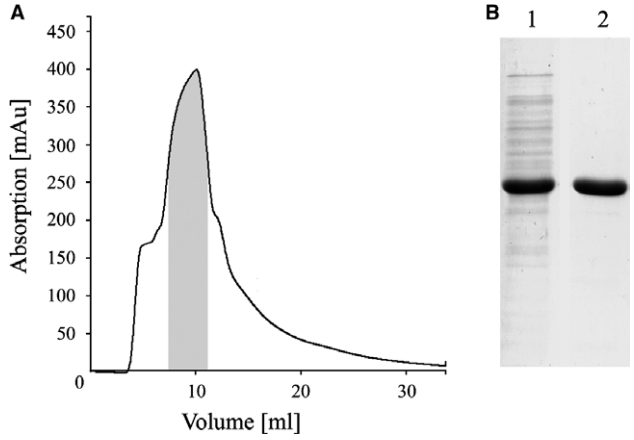

Fig. 1. Purification of *S. cerevisiae* subunit C (Vma5p). (A) Following purification of His6-Vma5p on Ni^{2+}–NTA resin, the protein was applied onto a RESOURCE™ Q column using Buffer A (50 mM Tris/HCl, pH 8.5, 150 mM NaCl, and 1 mM DTT) at a flow rate of 6 ml/min, followed by a gradient program 0 to 10% buffer B (Tris/HCl, pH 8.5, 1 M NaCl and 1 mM DTT (not shown)). Subunit C eluted already after 8–11 min and the contaminations eluted by increasing amounts of NaCl (not shown). (B) Lane 1 of an SDS-gel shows a sample of the His6-Vma5p after purification on Ni^{2+}–NTA resin. Lane 2, 20 μl of the indicated (▩) fractions was applied on the gel (lane 2).

3.2. Physical characterization of subunit C (Vma5p)

Treatment of subunit C with trypsin resulted in the formation of a 43 kDa species whose further degradation was slow (Fig. 2A). This implies that subunit C has a folded structure resistant to proteolytic degradation in vivo. The secondary structure of this subunit was determined from CD spectra, measured between 190 and 250 nm (Fig. 2B). The minima at 220 and 208 nm and the maximum at 192 nm indicate the presence of α-helical structures in the protein. Two computer-based methods were used to analyze the CD spectrum of subunit C. The average secondary structure content was 64% α-helix and 17% β-sheet.

3.3. Determination of molecular mass and overall dimensions of the native C subunit (Vma5p)

In order to determine the native MM of subunit C (Vma5p), a Superdex 75 gel filtration column was calibrated by determining the K_{av} values for a set of standard proteins of known MM. A calibration curve based on these K_{av} values is shown in Fig. 3. Comparison of the K_{av} for subunit C versus the standard proteins suggests the native molecular mass of approximately 51 ± 3 kDa. In a complementary approach, SAXS patterns from solutions of subunit C were recorded and processed as described in Section 2 to yield the final composite

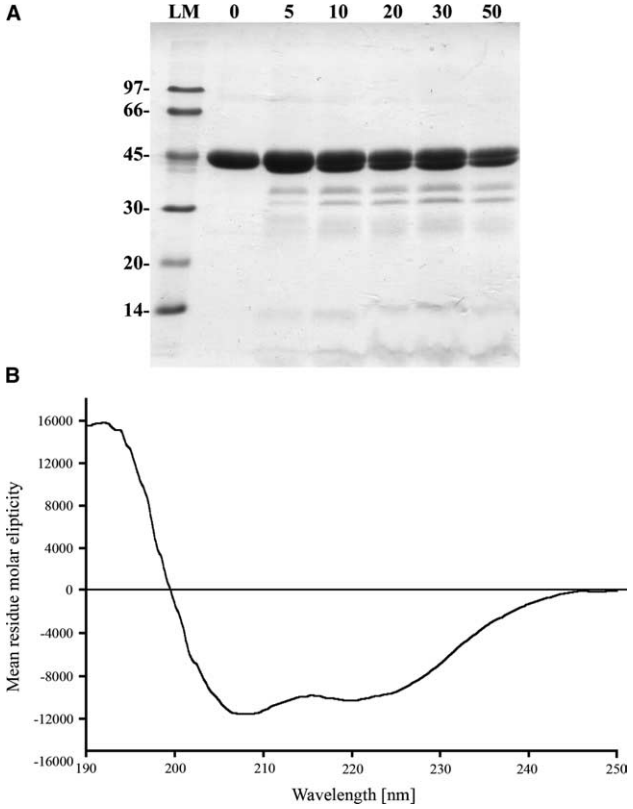

Fig. 2. Trypsin digestion and CD spectrum of subunit C (Vma5p). (A) Subunit C was incubated with trypsin at a ratio of 900:1 (w/w) for the indicated time. At the time indicated, aliquots were removed and the protease inhibitor Pefabloc SC was added to a final concentration of 8 mM. SDS sample buffer was added and the samples were electrophoresed on a 17.5% total acrylamide and 0.4% cross-linked acrylamide gel and stained with Coomassie Blue G250. Each lane received 6 μg of protein. (B) The CD spectrum of subunit C was determined using a Jasco-715 spectropolarimeter.

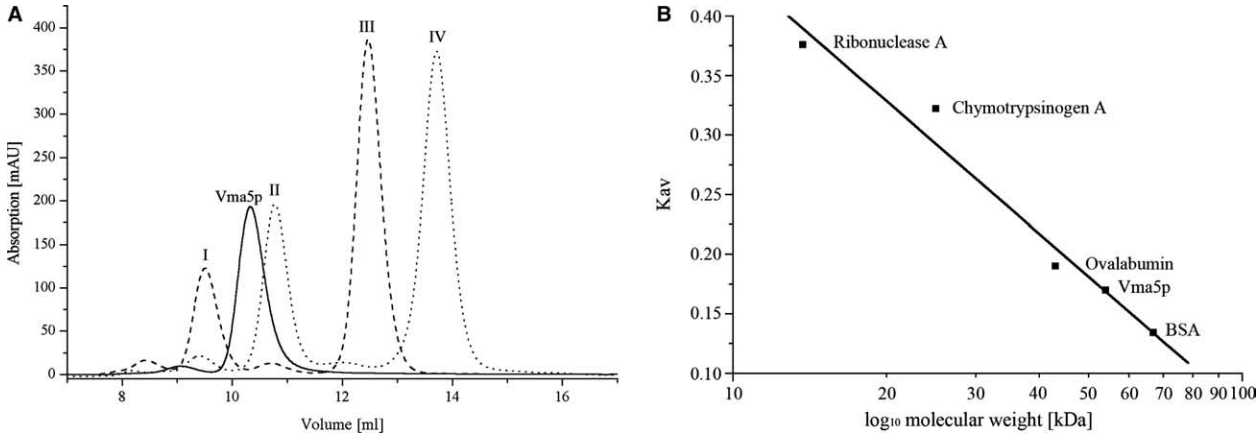

Fig. 3. Determination of native molecular mass by gel filtration analysis. (A) Superdex 75 gel filtration analysis of subunit C was performed as described under Section 2. Proteins used as molecular size standards (◆) were BSA (I, 67 kDa), ovalbumin (II, 45 kDa), β-chymotrypsin A (III, 25 kDa) and ribonuclease A (IV, 13.7 kDa). (B) For each protein, a K_{av} parameter was derived as described under Section 2. The K_{av} for subunit C (Vma5p) is indicated by (■).

scattering curve in Fig. 4. The radius of gyration R_g and the maximum dimension D_{max} of subunit C are 3.74 ± 0.03 and 12.5 ± 0.1 nm, respectively, suggesting that the subunit is a rather elongated particle. Comparison with the scattering from the reference solutions of BSA yields the estimate of MM of 51 ± 4 kDa, in agreement with the results of the gel filtration chromatography and indicating that subunit C is monomeric at the concentrations used. However, the determined MM of the native molecule is somewhat larger than expected from the denaturated protein (about 45 kDa, see Fig. 2) and the amino acid sequence (44 849 Da; Expert Protein Analysis System [37]). This may be attributed to a high hydration of the particle in solution, characteristic for extended molecules with large specific surface accessible to the solvent. The excluded (Porod) volume of the hydrated particle in solution was 100 ± 5 nm^3 (compared to the dry particle volume of 54 nm^3 computed from the sequence) also suggesting rather high hydration of subunit C. The distance distribution function $p(r)$ (Fig. 4, insert) further confirms that subunit C is an elongated particle with the average radius of cross-section of about 3 nm as reflected by the main maximum of the $p(r)$ function. The shoulder at larger intraparticle distances indicates that the particle consists of two distinct domains with the average distance between their centers of about 8 nm.

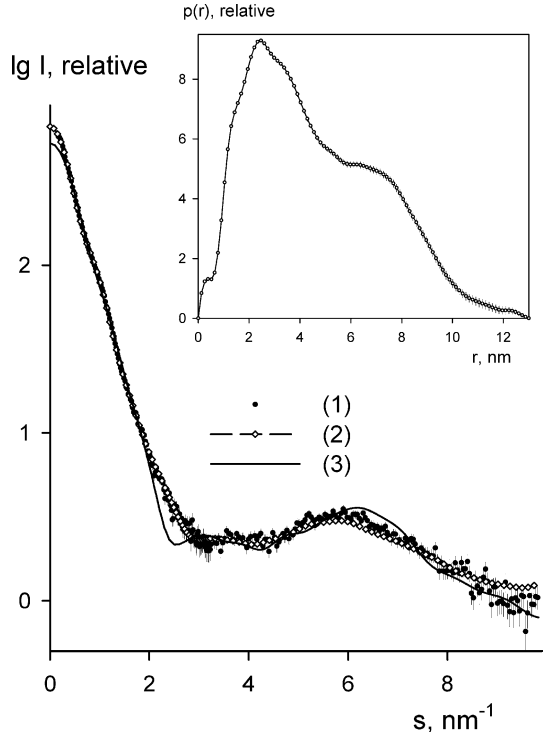

Fig. 4. X-ray scattering patterns from subunits C (Vma5p) and H (Vma13p) of yeast V-ATPase. (1) Experimental SAXS curve from subunit C; (2) scattering from typical ab initio model of subunit C computed by the program GASBOR [30]; (3) scattering pattern from the high resolution model of subunit H ([12] PDB code 1HO8) calculated by the program CRYSOL [34]. The distance distribution function of subunit C computed from the experimental data by the program GNOM [26] is displayed in the inset.

3.4. Shape and domain structure of subunit C (Vma5p)

The gross structure of subunit C was restored ab initio from the scattering pattern in Fig. 4 using the shape determination program DAMMIN and the dummy residues modeling program GASBOR as described in Section 2. The two approaches yielded similar results but the models provided by DAMMIN could only fit the data up to $s = 0.25$ nm^{-1} and therefore resulted in lower resolution. In the following, the models obtained with GASBOR are presented, which yield good fits to the experimental data in the entire scattering range (a typical fit displayed in Fig. 4, curve 2, has the discrepancy $\chi = 1.39$). Twelve independent reconstructions yielded reproducible models and the average model and the most probable model are displayed in Fig. 5 (left and middle columns, respectively). Subunit C appears as an elongated boot-shaped molecule with two distinct domains. This gross structure resembles very much the shape of subunit H (Vma13p; Fig. 5, right column) available in the PDB (33) (entry 1HO8). Moreover, the scattering pattern computed from the model of subunit H displays a fair agreement to the scattering by the subunit C in the entire range of scattering angles (Fig. 4, curve 3, $\chi = 2.5$). Some systematic deviations observed at the very small angles point to a somewhat more extended appearance (or, possibly, a higher hydration) of the subunit C than of the subunit H, but

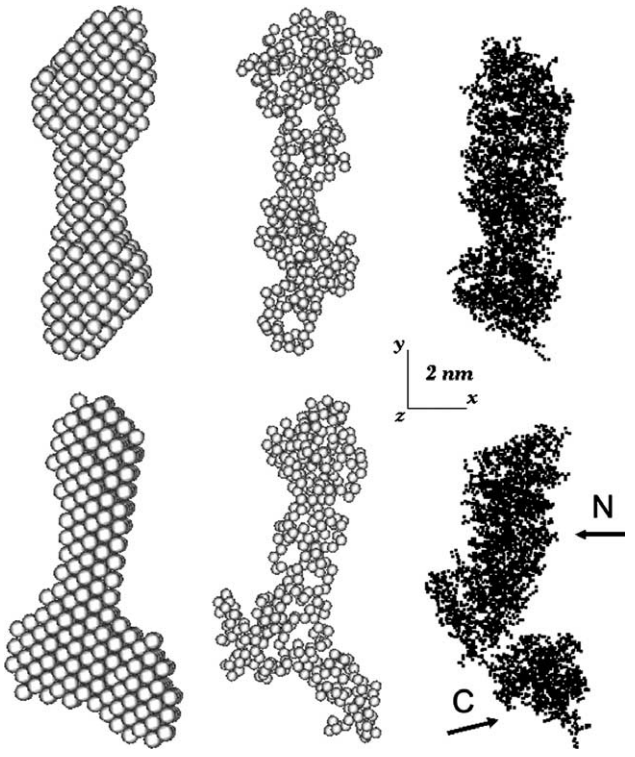

Fig. 5. Models of the subunits C and H from yeast V-ATPase. Left column and middle columns: averaged and most probable models of subunit C displayed as beads and dummy residues, respectively. Right column: high resolution model of subunit H ([12] PDB code 1HO8); the N- and C-termini are indicated by arrows. Models in the bottom row are rotated counterclockwise by 90° around the *y*-axis. The models were aligned using the program SUPCOMB [32] and displayed on an SGI workstation using the program ASSA [48].

the overall resemblance is still remarkable. Moreover, a good correlation is observed between the predicted scattering from subunit H and the experimental scattering from subunit C at higher angles ($4 < s < 9$ nm^{-1}), i.e., in the resolution range responsible for the internal domain organization and tertiary structure [38]. These results suggest that subunit H (Vma13p) and subunit C (Vma5p) not only display the same overall appearance but also have similar domain and possibly tertiary structure, although the two subunits show a sequence similarity and identity of only 34% and 17%, respectively (Fig. 6).

3.5. Assembly of subunit C (Vma5p) with V_1(-C) from M. sexta

Recent data using a chimeric yeast V-ATPase with subunit C from mouse demonstrated that subunit C is related to the energy coupling [39]. This chimeric formation prompted us to examine whether a hybrid of subunit C (Vma5p) and the V_1 ATPase without C (V_1(-C)) from *M. sexta*, whose C subunit seems to be released into the cytoplasm in the process of V_1V_O dissociation [40], can be formed. The analysis of such a hybrid complex is helpful in determining the function of the C subunit in ATPase activity. To test whether a V_1(-C)–Vma5p complex can be formed, the V_1(-C) complex from *M. sexta* together with subunit C (Vma5p) from yeast was incubated overnight. The subsequent size-exclusion chromatography resulted in an exclusion diagram with the three main peaks at 9, 12 and 27 ml (Fig. 7A). The fractions of these peaks were pooled, concentrated and analyzed by SDS–PAGE (Fig. 7B). The recovered peak I comprises the subunits of V_1(-C) plus subunit C (Vma5p) in stoichiometric amounts. Peak II contains V_1(-C) and subunit C (Vma5p) elutes as peak III. The V_1(-C)–Vma5p complex (peak I) and the V_1(-C) showed ATPase activity of 2.4 ± 0.1 U/ml and 1.9 ± 0.1 μmol U/ml, respectively.

```
Vma13p   1   MGATKILMDS THFNEIRSII RSRSVAWDAL ARSEELSEID ASTAKALESI  50
Vma5p    1   --------MA T------ALY TANDFIL--I SLPQNAQPVT APGSKT-DSW  33

Vma13p  51   LVKKNIGDGL SSSNNAHSGF KVNGKTLIPL IHLLSTSDNE DCKKSVQNLI 100
Vma5p   34   FNETLIGGRA FVSDFKIPEF KI-G-S---- LDTLI-VESE ELSK-VDN--  73

Vma13p 101   AELLSSDKYG DDTVKFFQED PKQLEQLFDV SLKGDFQTVL ISGFNVVSLL 150
Vma5p   73   -Q-I-----G ASIGKII--E I--LQGLNET STNA-YRTLP INNMPVPEYL 111

Vma13p 151   VQNGLHNVKL -VEKLLKNNN LINILQNIEQ MDTCYVCIRL LQELAVIPEY 199
Vma5p  112   ENFQWQTRKF KLDKSIK--D LITLISN--- ---------- --ESSQLDA- 143

Vma13p 200   RDVIWLHEKK FMPTLFKILQ RATDSQLATR IVATNSNHLG IQLQYHSLLL 249
Vma5p  143   -DV------- ------RATY -ANYNSAKTN LAAAERKKTG -DLSVRSLHD 177

Vma13p 250   IWLLTFNEV- FANELVQKYL SDFLDLL-KL VKITIKEKVS RLCISIILQC 297
Vma5p  177   --IV--KEED FVLN--SEHL TTVLVAVPKS LKSDFEKSYE TLSKNVVPAS 221

Vma13p 298   CSTRVKQHKK VIKQLLLLGN ALPTVQSLSE RKYSDEELRQ DISNLKEILE 347
Vma5p  222   ASVIAEDAEY VLFNVHLFKK NVQEFTTAAR EKKF---IPR EF-NYSEELI 267

Vma13p 348   NEYQELTSFD EYVAELDSKL LCWSPPHVDN GFWSDNIDEF KKDNYKIFRQ 397
Vma5p  267   -D--QLKKEH DSAASLEQSL RVQL---VRL AK-TAYVDVF --INWFHIKA 308

Vma13p 398   LIELLQAKVR NGDVNAKQEK IIIQVALNDI THVVELLPES IDVLDKTGGK 447
Vma5p  309   LRVYVESVLR YGLPPHFNIK -IIAVPPKNL S---KCKSEL IDAFGFLGGN 354

Vma13p 448   A---DIMELL NHSDSRV-KY EALKAT--QA IIGYTFK- 478
Vma5p  355   AFMKDKKGKI NKQLTSLHQY ASLVDTEYEP FVMYIINL 392
```

Fig. 6. Sequence alignment of Vma5p and Vma13p. Alignment was generated using BioEdit 5.0.9 Sequence Alignment Editor [49]. Identical and homologous amino acids are highlighted in black and gray shading, respectively.

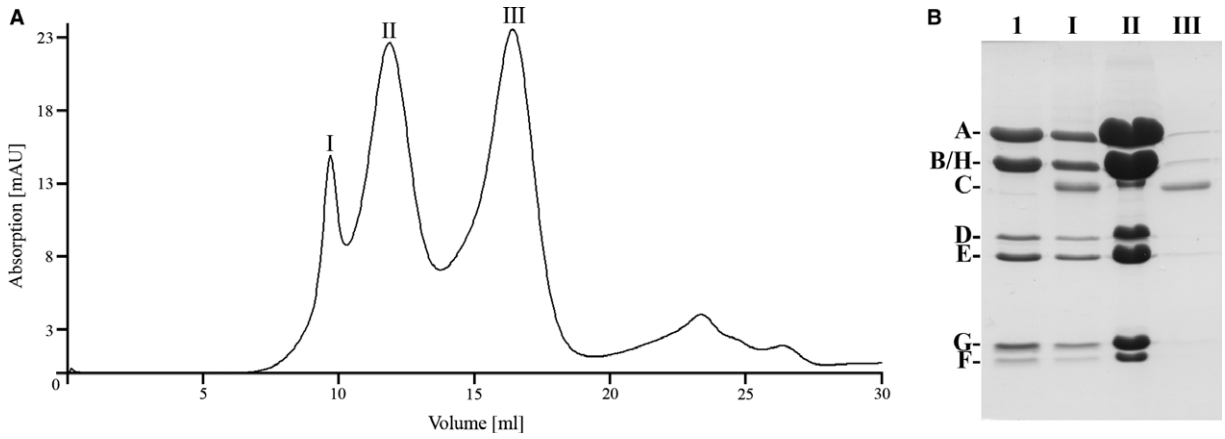

Fig. 7. Elution profile and electrophoretic analysis of the assembled V_1(-C)-ATPase from *M. sexta* and subunit C (Vma5p). (A) V_1(-C)-ATPase from *M. sexta* and subunit C (Vma5p) was incubated as described in Section 2 and applied onto a Sephacryl S-300 HR column with 20 mM Tris/HCl (pH 8.1), and 150 mM NaCl. (B) The fractions of peaks I, II and III were pooled, concentrated and subjected to a gradient SDS–PAGE. The gel was stained with Coomassie blue G250.

4. Discussion

The function of the stalk subunit C of V_1V_O ATPases is still elusive. For the H^+-ATPase of clathrin-coated vesicles, it has been demonstrated that the addition of recombinant subunit C to an A_3B_3E complex significantly increased the ATPase activity [41]. Genetic and biochemical data suggest that subunit C is essential in regulation and stabilization of V_1V_O interaction [11,40,42]. From recent studies using crosslinkers it has been shown that subunit C is in close neighborhood to subunit E [43], the latter of which is in close proximity to the stalk subunit D [43,44], and in contact with subunit c of the V_O part [45]. As estimated from electron micrographs of negatively stained V_1(-C) ATPase from *M. sexta* [7], the stalk is about 6 nm in height and shorter than the value of 11 nm determined by the hydrated V_1 ATPase using SAXS [6]. It has been argued that this difference may have been caused by a dissociation of the C subunit from the stalk at the low concentrations necessary for electron microscopy [7]. A length of about 12.5 nm of the hydrated C subunit (Vma5p) as determined in the presented studies would exceed the distance of 11 nm. Taken together, these data imply that the peripheral stalk subunit C might span the length of the stalk thereby linking the V_1 and V_O domains. It is of particular interest that the V_1V_O disassembly is accompanied by the dissociation of subunit C from the complex [3,40], and it has been hypothesized that subunit C plays a central role in the reversible reassembly of both domains [3,40] by binding as an anchor protein to the actin-based cytoskeleton and controlling the linkage of the cytoplasmic V_1 complex with the actin filaments [40]. The presented elongated envelope of subunit C (Vma5p), consisting of two distinct domains (Fig. 5), would provide interfaces to interact with other V_1, V_O subunits and F-actin. Its boot-shaped structure, consisting of two distinct domains, is remarkably similar in its overall structure to that of subunit H (Vma13p), composed of an elongated bootleg, made up by the N-terminal domain (Fig. 5) and a foot, which is formed by the C-terminal domain. Both domains are connected by a flexible linker [12]. The C-terminal half of subunit H is proposed to bind to the V-ATPase subunits [13,43], whereby the long terminal shaft interacts with proteins like Ynd1p [46] or the Nef-binding protein-1 [47]. In comparison, the C-terminus of subunit C (Vma5p), which includes the most highly conserved region of this subunit, appears to be very important for stable assembly of V_1V_O. Mutagenesis of this region reduced ATPase activity in vitro, because of loss of V_1 subunits [42], indicating that subunit C might also be in contact with the V_1 subunits via its C-terminal domain. Although the structural similarities of the C and H subunits are significant, presently we can only speculate about the bootleg shaped part of subunit C forming the binding domain of the oligomeric F-actin. However, both subunits have been viewed as components structurally and functionally bridging V_1 and V_O. Furthermore, it has been proposed that release of subunit C (Vma5p) from V_1 could play a role, in cooperation with subunit H (Vma13p) inhibition, in the silencing of MgATP hydrolysis in the disassembled V_1 part [11]. In this context, it is of interest that the V_1(-C) complex from *M. sexta* has an ATPase activity which is 20% lower compared to the reconstituted V_1-Vma5p hybrid complex.

In summary, the data presented demonstrate that subunit C of the yeast vacuolar ATPase exists in solution as an elongated molecule, organized as two well-defined domains, as determined by two ab initio shape restoration procedures. The similarity in shape of both subunit C (Vma5p) and H (Vma13p) is in line with their function in bridging the V_1 and V_O parts. These findings will allow a better understanding of the structural and functional role(s) of subunit C within the V_1V_O complex.

Acknowledgements: We thank Dr. W. Nastainczyk (Universität des Saarlandes) for amino acid sequencing and Dr. B. Schiffler for his support in CD measurements (Universität des Saarlandes). This research was supported by a grant from the Deutsche Forschungsgemeinschaft (GR 1475/9-1 and GR 1475/9-2).

References

[1] Graham, L.A., Flannery, A.R. and Stevens, T.H. (2003) J. Bioenerg. Biomembr. 35, 301–312.
[2] Nelson, N. (2003) J. Bioenerg. Biomembr. 35, 281–290.
[3] Kane, P.M. and Smardon, A.M. (2003) J. Bioenerg. Biomembr. 35, 313–322.
[4] Xu, T., Vasilyeva, E. and Forgac, M. (1999) J. Biol. Chem. 274, 28909–28915.

[5] Nishi, T. and Forgac, M. (2002) Natl. Rev. Mol. Cell Biol. 3, 94–103.
[6] Svergun, D.I., Konrad, S., Huss, M., Koch, M.H.J., Wieczorek, H., Altendorf, K., Volkov, V.V. and Grüber, G. (1998) Biochemistry 37, 17659–17663.
[7] Radermacher, M., Ruiz, T., Wieczorek, H. and Grüber, G. (2001) J. Struct. Biol. 135, 26–37.
[8] Sumner, J.P., Dow, J.A.T., Earley, F.G., Klein, U., Jäger, D. and Wieczorek, H. (1995) J. Biol. Chem. 270, 5649–5653.
[9] Kane, P.M. (1995) J. Biol. Chem. 270, 17025–17032.
[10] Trombetta, E.S., Ebersold, M., Garrett, W., Pypaert, M. and Mellman, I. (2003) Science 299, 1400–1403.
[11] Curtis, K.K. and Kane, P.M. (2002) J. Biol. Chem. 277, 2716–2724.
[12] Sagermann, M., Stevens, T.H. and Matthews, B.W. (2001) Proc. Natl. Acad. Sci. USA 98, 7134–7139.
[13] Landolt-Marticorena, C., Williams, K.M., Correa, J., Chen, W. and Manolson, M.F. (2000) J. Biol. Chem. 275, 15449–15457.
[14] Iwata, M., Imamura, H., Stambouli, E., Ikeda, C., Tamakoshi, M., Nagata, K., Makyio, H., Hankamer, B., Barber, J., Yoshida, M., Yokoyama, K. and Iwata, S. (2003) Proc. Natl. Acad. Sci. USA 101, 59–64.
[15] Yokoyama, K., Nagata, K., Imamura, H., Ohkuma, S., Yoshida, M. and Tamakoshi, M. (2003) J. Biol. Chem. 278, 42686–42691.
[16] Laemmli, U.K. (1970) Nature 227, 680–685.
[17] Matsudaira, P. (1987) J. Biol. Chem. 262, 10035–10038.
[18] Provencher, S.W. (1982) Comput. Phys. Commun. 27, 213–227.
[19] Andrade, M.A., Chacon, P., Merelo, J.J. and Moran, F. (1993) Protein Eng. 6, 383–390.
[20] Boulin, C., Kempf, R., Koch, M.H.J. and McLaughlin, S.M. (1986) Nucl. Instrum. Methods A 249, 399–407.
[21] Boulin, C.J., Kempf, R., Gabriel, A. and Koch, M.H.J. (1988) Nucl. Instrum. Methods A 269, 312–320.
[22] Gabriel, A. and Dauvergne, F. (1982) Nucl. Instrum. Methods 201, 223–224.
[23] Konarev, P.V., Volkov, V.V., Sokolova, A.V., Koch, M.H.J. and Svergun, D.I. (2003) J. Appl. Crystallogr. 36, 1277–1282.
[24] Svergun, D.I. (1993) J. Appl. Crystallogr. 26, 258–267.
[25] Guinier, A. (1939) Ann. Phys. (Paris) 12, 161–237.
[26] Svergun, D.I. (1992) J. Appl. Crystallogr. 25, 495–503.
[27] Svergun, D.I. (1999) Biophys. J. 76, 2879–2886.
[28] Kirkpatrick, S., Gelatt Jr., C.D. and Vecci, M.P. (1983) Science 220, 671–680.
[29] Porod, G. (1982) General theory. in: Small-angle X-ray Scattering (Glatter, O. and Kratky, O., Eds.), pp. 17–51, Academic Press, London.
[30] Svergun, D.I., Petoukhov, M.V. and Koch, M.H.J. (2001) Biophys. J. 80, 2946–2953.
[31] Volkov, V.V. and Svergun, D.I. (2003) J. Appl. Crystallogr. 36, 860–864.
[32] Kozin, M.B. and Svergun, D.I. (2001) J. Appl. Crystallogr. 34, 33–41.
[33] Berman, H.M., Westbrook, J., Feng, Z., Gilliland, G., Bhat, T.N., Weissig, H., Shindyalov, I.N. and Bourne, P.E. (2000) Nucleic Acids Res. 28, 235–242.
[34] Svergun, D.I., Barberato, C. and Koch, M.H.J. (1995) J. Appl. Crystallogr. 28, 768–773.
[35] Rizzo, V.F., Coskun, Ü., Radermacher, M., Ruiz, T., Armbrüster, A. and Grüber, G. (2003) J. Biol. Chem. 278, 270–275.
[36] Lötscher, H.-R., de Jong, C. and Capaldi, R.A. (1984) Biochemistry 23, 4140–4143.
[37] Gasteiger, E., Gattiker, A., Hoogland, C., Ivanyi, I., Appel, R.D. and Bairoch, A. (2003) Nucleic Acids Res. 31, 3784–3788.
[38] Sokolova, A.V., Volkov, V.V. and Svergun, D.I. (2003) J. Appl. Crystallogr. 36, 865–868.
[39] Sun-Wada, G.-H., Murata, Y., Namba, M., Yamamoto, A., Wada, Y. and Futai, M. (2003) J. Biol. Chem. 278, 44843–44851.
[40] Vitavska, O., Wieczorek, H. and Merzendorfer, H. (2003) J. Biol. Chem. 278, 18499–18505.
[41] Peng, S.B., Zhang, Y., Tsai, S.J., Xie, X.S. and Stone, D.K. (1994) J. Biol. Chem. 269, 11356–11360.
[42] Curtis, K.K., Francis, S.A., Oluwatosin, Y. and Kane, P.M. (2002) J. Biol. Chem. 277, 8979–8988.
[43] Xu, T., Vasilyeva, E. and Forgac, M. (1999) J. Biol. Chem. 274, 28909–28915.
[44] Coskun, Ü., Rizzo, V.F., Koch, M.H.J. and Grüber, G. (2004) J. Bioenerg. Biomembr. 36, 249–256.
[45] Adachi, I., Arai, H., Pimental, R. and Forgac, M. (1990) J. Biol. Chem. 265, 960–966.
[46] Zhong, X., Malhotra, R. and Guidotti, G. (2000) J. Biol. Chem. 275, 35592–35599.
[47] Lu, X., Yu, H., Liu, S.H., Brodsky, F.M. and Peterlin, B.M. (1998) Immunity 8, 647–656.
[48] Kozin, M.B., Volkov, V.V. and Svergun, D.I. (1997) J. Appl. Crystallogr. 30, 811–815.
[49] Hall, T.A. (1999) Nucleic Acids Symp. Ser. 41, 95–98.